Marine Pollution Bulletin 233 (2026) 120338

Contents lists available at ScienceDirect

Marine Pollution Bulletin

journal homepage: www.elsevier.com/locate/marpolbul

Speciation of gadolinium-based contrast agents in wastewater and seawater: a case study in the northern Adriatic Sea

Claudia Stevanin [a], Tatiana Chenet [a,*], Elena Ciuffreda [a], Cinzia Fabbro [b], Mirco Cescon [a], Michele Giani [b], Valentina Costa [c], Luisa Pasti [a]

[a] Department of Environmental and Prevention Sciences, University of Ferrara, Via Luigi Borsari 46, 44121, Ferrara, Italy
[b] National Institute of Oceanography and Applied Geophysics – OGS, via A. Piccard 54, 34151, Santa Croce, Trieste, Italy
[c] Department of Chemical, Pharmaceutical and Agricultural Sciences, University of Ferrara, Via Luigi Borsari 46, 44121, Ferrara, Italy

ARTICLE INFO

Keywords:
Gadolinium-based contrast agents
Total gadolinium
Emerging contaminants
Speciation
Wastewater
Seawater
HPLC-ICP-MS

ABSTRACT

Coastal environments receiving treated municipal wastewater are increasingly exposed to anthropogenic gadolinium derived from gadolinium-based contrast agents (GBCAs). However, information regarding the occurrence and fate of individual GBCAs in Mediterranean marine waters remains scarce. This study investigated total gadolinium and GBCA speciation in raw and treated wastewater from an advanced wastewater treatment plant and in the receiving waters of the Gulf of Trieste (northern Adriatic Sea). Analysis of raw and treated wastewater revealed low overall Gd removal efficiencies (~24%), confirming that tertiary treatment processes fail to prevent GBCA discharge. High-performance liquid chromatography coupled with inductively coupled plasma mass spectrometry (HPLC–ICP-MS) identified the macrocyclic complexes gadoteridol (Gd-HP-DO3A) and gadoterate (Gd-DOTA) as the predominant GBCAs, with Gd-HP-DO3A accounting, on average, for over 60% of total Gd (Gd_{tot}) in wastewater. An optimised solid-phase extraction (SPE) sample preparation procedure using porous carbon enabled the first determination of individual GBCAs in high-salinity Mediterranean seawater. In the Gulf of Trieste, Gd-HP-DO3A exhibited a widespread spatial and temporal presence. However, GBCAs accounted for only 2% to 37% of Gd_{tot} in seawater samples, indicating that natural riverine geogenic sources and unmonitored macrocyclic GBCAs constitute the remaining Gd fraction. These findings confirm that persistent macrocyclic GBCAs are efficiently transferred from wastewater to Mediterranean coastal ecosystems, establishing anthropogenic Gd (Gd_{anth}) and specific GBCA species as robust molecular tracers of wastewater effluent dispersion.

1. Introduction

Contaminants of emerging concern (CECs) comprise a continuously expanding group of substances increasingly detected in aquatic environments due to their widespread use and persistence (Pastorino and Ginebreda, 2021). Among them, gadolinium-based contrast agents (GBCAs), extensively employed in magnetic resonance imaging (MRI), have attracted growing attention because of their increasing environmental occurrence (Ebrahimi and Barbieri, 2019; Rogowska et al., 2018; Scarciglia et al., 2025). Gadolinium is administered as highly stable chelates to prevent the toxicity associated with free Gd^{3+} ions. Following MRI examinations, GBCAs are excreted largely unchanged and enter municipal sewer systems, where their high chemical stability hinders their removal during conventional wastewater treatment (Inoue et al., 2022; Kesava Raju et al., 2010; Laczovics et al., 2023; Zabrecky et al., 2021). As a consequence, anthropogenic gadolinium (Gd_{anth}) derived from GBCAs is continuously discharged into rivers, groundwater and coastal waters, where positive gadolinium anomalies have been reported worldwide (Altomare et al., 2020; Amorim et al., 2019; Brünjes et al., 2016; Brünjes and Thilo Hofmann, 2020; Gao et al., 2025; Kraemer et al., 2024; Krohn et al., 2024; Kumasaka et al., 2024; Wysocka et al., 2023; Zhang et al., 2026). Recent studies, including the monitoring of the Tone River (Japan), have demonstrated a continuous increase in anthropogenic Gd associated with the growing use of MRI contrast agents (Kumasaka et al., 2024). Given their high chemical persistence and resistance to conventional wastewater treatment, their concentrations in aquatic environments are expected to further increase (Inoue et al., 2025; Oluwasola et al., 2022). The Mediterranean Sea is particularly vulnerable to anthropogenic Gd inputs because it receives wastewater and river discharges from densely populated coastal areas.

* Corresponding author.
E-mail address: tatiana.chenet@unife.it (T. Chenet).

https://doi.org/10.1016/j.marpolbul.2026.120338
Received 23 June 2026; Received in revised form 28 August 2026; Accepted 4 September 2026
Available online 8 September 2026
0025-326X/© 2026 The Authors. Published by Elsevier Ltd. This is an open access article under the CC BY license (http://creativecommons.org/licenses/by/4.0/).

Italy represents one of the major European contributors of anthropogenic Gd to the Mediterranean basin (Pereto et al., 2023), while the northern Adriatic Sea is especially sensitive owing to its shallow waters, limited water exchange and intense anthropogenic pressure (Fanelli et al., 2022). The environmental relevance of GBCAs is further supported by growing evidence that gadolinium species can bioaccumulate in aquatic organisms and induce adverse biological effects, including oxidative stress, developmental alterations and tissue accumulation (Martino et al., 2017; Lachaux et al., 2022, 2023; Andrade et al., 2023; Zhang et al., 2025; Moreira et al., 2025, 2026).

Although total gadolinium is widely recognised as a reliable tracer of wastewater-derived contamination, the determination of individual GBCAs provides more detailed information on contaminant sources, environmental behaviour and potential ecological risks. However, the occurrence and distribution of individual GBCAs in marine waters remain largely unexplored because of the analytical challenges associated with saline matrices. To the best of our knowledge, only one study has reported the determination of GBCAs in seawater (Horstmann et al., 2021), and no information is currently available for the Mediterranean Sea.

Therefore, the objectives of this study were to investigate the occurrence of total gadolinium and individual GBCAs in wastewater and in the receiving marine waters of the Gulf of Trieste (northern Adriatic Sea), to optimise an analytical method for GBCA speciation in seawater, and to provide the first evidence of the occurrence of these compounds in the Mediterranean Sea.

2. Materials and methods

2.1. Study area

The Gulf of Trieste (GoT) is a shallow (<25 m), semi-enclosed basin located in the northernmost part of the Adriatic Sea, covering an area of about 500 km^2 (Fig. 1). This embayment is in part isolated from the rest of the northern Adriatic Sea by a shoal along the direction from southeast to northwest from the Istria peninsula to the Grado-Marano lagoon (Faganeli et al., 2023) and collects waters from different rivers and wastewaters plants which may lead to contaminants input in the gulf ecosystem (Cozzi et al., 2012, 2014, 2020). The main freshwater input in the GoT comes from the Isonzo (Soča) and the Timavo rivers, in the north-western part of the basin (mean discharge between 1998 and 2008 = 82 and 27 m^3 s^{-1}, respectively) (Cozzi et al., 2012), while freshwater runoff from the Rosandra, Rižana and Dragonja streams in the eastern part is of torrential nature (Comici and Bussani, 2007) and provides only a minor contribution (Covelli et al., 2025). The river runoff shows a wide interannual variability (Comici and Bussani, 2007; Savonitto et al., 2025) and affects surface salinity, whose values range from 32 to 38 (Malačič et al., 2006). In addition to the buoyancy effects of the Isonzo River plume, the hydrodynamics of the GoT are controlled by tides, the intense local wind regime, characterised by the alternance of cold and dry north-easterly winds (i.e., Bora) with milder southeasterly winds (i.e., Scirocco), and by water masses exchanges with the Adriatic Sea (Falcieri et al., 2016). The GoT is influenced by the currents flowing northwards along the Istrian coast, which induce a general circulation characterised by a main cyclonic gyre, daily modulated by the local wind field. The vertical structure of currents is decoupled with two independent upper (surface - 5 m) and lower (10 m - bottom) layers, and an intermediate transition layer in between. The

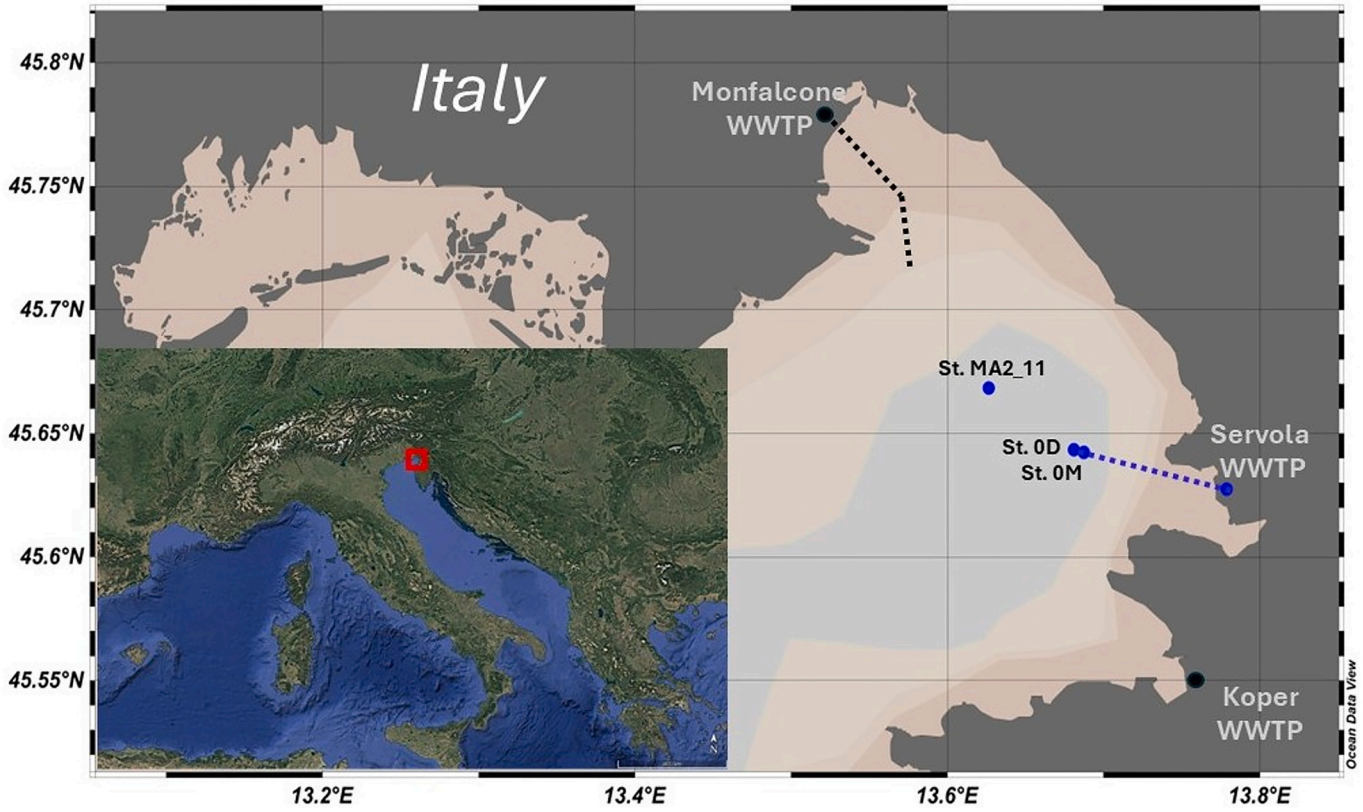

Fig. 1. Map of the sampling sites in the Gulf of Trieste (northern Adriatic Sea). Blue dots indicate wastewater and seawater sampling stations, whereas black dots indicate the locations of the WWTP of Monfalcone and Koper. (For interpretation of the references to colour in this figure legend, the reader is referred to the web version of this article.)

upper layer is mainly wind-driven, while the lower layer follows the general cyclonic circulation of the northern Adriatic Sea (Querin et al., 2007 and references therein). The GoT hosts three main coastal urban cities - Trieste, Koper and Monfalcone - with a combined population of approximately 280,000 inhabitants, served by wastewater treatment systems. Treated effluents from Trieste and Monfalcone are discharged into the sea through marine outfalls, while in Koper treated wastewater flows into the Rižana River just before it reaches the sea (Krzyk et al., 2024). The Servola wastewater treatment plant (WWTP), serving the city of Trieste, is the largest sewage treatment facility in the study area. This plant is located in the north-eastern part of the GoT, serving approximately 190,000 population equivalents (p.e.). The WWTP is fed by a combined sewer system, in which domestic and industrial wastewater is conveyed together with wet-weather inflows. Consequently, influent flow and composition may vary according to antecedent rainfall conditions. Average treated flows are on the order of 100,000–125,000 m^3 day^{-1} (mean values for the years 2021–2023), corresponding to roughly 40 $*10^6$ m^3 of treated wastewater annually. Following the 2018 upgrade, the Servola WWTP was converted from mainly physico-chemical treatment to a full advanced system with primary, secondary, and tertiary treatment, including UV disinfection. The treated effluent is conveyed offshore through a 7.5 km long submarine pipeline, the last 1.5 km of which, located at a depth between 20 and 23 m, are equipped with a diffuser system that enhances dilution.

2.2. Chemicals and consumables

Gadolinium based contrast agents (GBCAs), gadopentetate monomeglumine (Gd-DTPA), gadoteridol (Gd-HP-DO3A) and gadoterate meglumine (Gd-DOTA), were purchased from Sigma Aldrich (Steinheim, Germany). Methanol, ammonium nitrate, ammonia, hydrochloric acid, nitric acid, di(2-ethylhexyl)-phosphate (HDEHPA), acetonitrile and sodium carbonate were purchased from Sigma Aldrich, whereas deionised water was produced using a water purification system MilliQ (Millipore, MA, USA). The Multi-element Calibration Standard 1 solution containing the rare earth elements was purchased from Agilent (Agilent Technologies, Santa Clara, CA, USA). For the solid phase extraction sample treatment, prior to the determination of rare earth elements content, a Bond Elut C18 cartridge, 1 g, 6 mL, 40 μm, (Agilent Technologies, Santa Clara, CA, USA) was employed. Instead, CHROMABOND® Carbon A cartridges, 500 mg, 6 mL (Macherey-Nagel, Düren, Germany) with highly porous activated carbon were used to perform the speciation analyses of GBCAs. To avoid Gd and GBCAs adsorption on the vessels, only polypropylene or polyethylene materials were used during sampling and throughout sample treatment and analysis.

2.3. Sampling

Seawater sampling in the GoT was carried out during three campaigns conducted in August, October, and December 2023 at stations 0M, located in the central section of the diffuser system of the submarine outfall, and 0D, positioned at the end of the pipeline. A reference station (MA2_11), located in the central area of the GoT approximately 5 km from the outfall and with a similar water column depth, was also included (Fig. 1). Water samples were collected at the surface and near the bottom using Niskin bottles mounted on a rosette sampler triggered to close at the selected depths. Salinity and turbidity throughout the water column were recorded using an SBE 19plus CTD profiler (Sea-Bird Scientific, Bellevue, WA, USA). Raw and treated wastewater grab samples from the Servola WWTP were taken concurrently with the marine sampling campaigns. Seawater and wastewater aliquots (1 L) were transferred into polyethylene bottles and stored at temperature ≤ 6 °C until analysis. For total Gd determination, aliquots were stabilised with HCl (6 N) to a final pH of 2, whereas those intended for speciation analysis were kept unacidified to avoid degradation of GBCAs.

2.4. Sample treatment for total rare earth elements quantification

To determine the rare earth elements content, both wastewater and seawater samples were processed through solid phase extraction (SPE) to isolate the analyte while removing the major components of the matrix that would interfere during analysis. Before performing the extraction, the pH of the water sample was changed from 2 to 3.2 by adding 1 M Na_2CO_3 solution to ensure the efficient retention of all REEs on the complexing agent loaded on the SPE cartridge (di(2-ethylhexyl) phosphate), thereby achieving high recoveries (Shabani et al., 1992). The C18 cartridges were firstly conditioned with 10 mL of 6 M HCl, then they were washed with 10 mL of deionised MilliQ water, loaded with 500 μL of di(2-ethylhexyl) phosphate, washed with 10 mL of 6 M HCl, 10 mL of 0.1 M HCl, and finally with 10 mL of deionised MilliQ water. 200 mL of sample was loaded and processed, the cartridge was then washed with 10 mL 0.01 M HCl, then the elution was carried out with 15 mL of 6 M HNO_3. The samples collected were concentrated almost to dryness by heating at 70 °C in a water bath, then they were recovered with 10 mL of deionised MilliQ water (Hennebrüder et al., 2004). The samples were analysed by inductively coupled plasma mass spectrometry using an Agilent 8800 triple quadrupole ICP-MS (Agilent Technologies, Santa Clara, CA, USA). The instrumental conditions were 1550 W RF power, 8.0 mm sampling depth, 15 L min^{-1} plasma gas flow, 1.03 L min^{-1} carrier gas flow, spray chamber temperature 2 °C, reaction cell gas He, 5 mL min^{-1} reaction gas flow, 100 ms integration time, In and Re were used as internal standards. The following masses were monitored: ^{157}Gd, ^{158}Gd, ^{139}La, ^{140}Ce, ^{141}Pr, ^{145}Nd, ^{146}Nd, ^{147}Sm, ^{149}Sm, ^{151}Eu, ^{153}Eu, ^{159}Tb, ^{161}Dy, ^{163}Dy, ^{165}Ho, ^{166}Er, ^{167}Er, ^{169}Tm, ^{172}Yb, ^{173}Yb, ^{174}Yb, ^{175}Lu, ^{115}In, ^{187}Re. Before analysis, the ICP-MS was tuned using a multielement tuning solution (Agilent Technologies, Santa Clara, CA, USA); the oxide formation and double charge species formation were checked by monitoring CeO^+/Ce^+ ($\leq$1%) and Ce^{2+}/Ce^+ ($\leq$1%) ratios.

2.5. Sample treatment for speciation analyses

To investigate the presence of GBCAs in wastewater, the samples were treated through evaporation in mild conditions to avoid any analyte loss (Kesava Raju et al., 2010). 250 mL of sample were poured in a polypropylene beaker and concentrated to 2 mL in a water bath at 50 °C. The sample was then recovered to 5 mL with MilliQ water and filtered with a 0.2 μm PVDF syringe filter before the analysis.

Due to the complexity of the matrix, especially the high content of salts which can interfere with the analysis, the separation of the GBCAs from the seawater samples was carried out via SPE.

In this work SPE cartridges containing activated and highly porous carbon (Chromabond Carbon A) were employed. The SPE procedure was developed by modifications of the method proposed by Horstmann et al. (2021). The pH of the seawater samples was modified at 4 to increase the recovery; the SPE cartridge was conditioned with 20 mL of MilliQ water, then 250 mL of sample were loaded, the cartridge was washed with 10 mL of MilliQ water to remove any residual salt, then the analytes were eluted with 10 mL of a mixture of acetonitrile and MilliQ water in a ratio of 75:25. The sample was then concentrated under nitrogen flow, recovered to 5 mL with MilliQ water and filtered with a 0.2 μm PVDF syringe filter before the analysis.

2.6. GBCAs speciation analysis by HPLC-ICP-MS

The speciation analyses were carried out with a HPLC Agilent 1260 Infinity coupled to an ICP-MS Agilent 8800 Triple Quadrupole (Agilent Technologies, Santa Clara, CA, USA).

The separation was performed with the anion exchange column Dionex IonPac AS9-HC 250 mm length, 4 mm internal diameter, 9 μm particle diameter, equipped with the guard column Dionex IonPac AG9-HC (Thermo Fisher Scientific, Waltham, MA USA), the stationary phase of this column is characterised by quaternary ammonium alkyl groups.

The mobile phase was a 125 mM ammonium nitrate buffer solution at pH 9 prepared by dissolving NH_4NO_3 in deionised MilliQ water and adjusting the pH with 10% ammonia solution. The mobile phase was filtered before use with 0.45 μm nylon 66 membranes (Supelco, Bellefonte, PA, USA).

100 μL of solution, sample or standard, was injected by an autosampler system, and the mobile phase flow was kept at 1 mL min^{-1}.

The exit of the column was directly connected to the peristaltic pump of the ICP-MS through a 27.5 cm long PEEK tube to transfer the mobile phase flow into the nebuliser of the detection system. The length of the connecting tube was kept as short as possible mainly to avoid peak widening in the chromatogram.

The ICP-MS conditions were: 1550 W RF power, 8.0 mm sampling depth, 15 L min^{-1} plasma gas flow, 1.03 L min^{-1} carrier gas flow, spray chamber temperature 2 °C, reaction cell gas He, 5 mL min^{-1} reaction gas flow, 100 ms integration time, the masses monitored were ^{157}Gd and ^{158}Gd.

2.7. Quality assurance

For every procedure, recovery tests were performed from synthetic water matrices mimicking the real water samples and spiked with the analytes at a concentration of 10 ng L^{-1} to verify the efficiency of the method. For speciation analyses in seawater, recovery tests were performed at different pH values to optimise the sample treatment procedure.

For each sample treatment, procedural blanks were analysed to account for background contamination. The linearity of the analytical method ($R^2 > 0.999$) was verified using calibration standards in a concentration range that covered the concentrations expected in the samples (0.1–5000 ng L^{-1}).

The method limit of detection (LOD) for total Gd content analysis was 0.07 ng L^{-1}, whereas the LODs for the speciation investigation were 0.16 ng L^{-1}, 0.11 ng L^{-1} and 0.52 ng L^{-1} for Gd-HP-DO3A, Gd-DOTA and Gd-DTPA, respectively. The LOD of the other REE were within 0.005–0.08 ng L^{-1}.

Recoveries for each REE for wastewater and seawater matrices were between 87 and 102%.

A potential methodological limitation for total Gd determination is that samples were directly subjected to SPE without a prior oxidative pretreatment. Although the analytical protocol was based on the C18 combined with di(2-ethylhexyl) phosphate SPE method of Hennebrüder et al. (2004), recent work by Krohn et al. (2024) has shown that H_2O_2 oxidation prior to extraction may improve the determination of total Gd by promoting the decomposition of intact GBCAs. The influence of this additional pretreatment was not evaluated in the present study and therefore cannot be assessed. Future studies should investigate whether its implementation further improves total Gd recovery when using C18 combined with di(2-ethylhexyl) phosphate SPE.

For speciation analyses, recoveries for wastewater matrix were higher than 90% for each GBCAs, whereas for seawater matrix recoveries ranged between 75 and 79% at the optimised pH for Gd-HP-DO3A and Gd-DOTA, but less than 40% for Gd-DTPA (see the Results and Discussion sections). The analyses were carried out in triplicate.

3. Results

3.1. Gd anomaly in seawater, raw wastewater and treated wastewater

In the present study, the magnitude of the positive Gd anomaly was evaluated across the investigated water matrices as an initial assessment of potential Gd contamination. Concentrations of each rare earth element in the water samples were normalised to the REE content in the Post-Archean Australian Shale (PAAS), used as a proxy of average REE concentration in the upper continental crust (McLennan, 1989). Figs. S1-S3 report the REE/PAAS patterns in seawater, raw wastewater and treated wastewater samples.

A significant positive Gd anomaly was observed in the raw and treated wastewater collected in August 2023. The anomaly was less evident in the samples collected in October and December 2023, which also had lower Gd concentrations. Almost all analysed samples showed a positive gadolinium anomaly, although often at low intensity.

3.2. Speciation of gadolinium-based compounds

To further investigate the origin of the Gd anthropogenic contribution, a speciation study was performed. Three GBCAs were considered: a linear GBCA (gadopentetate monomeglumine Gd-DTPA) and two macrocyclic GBCAs (gadoteridol Gd-HP-DO3A and gadoterate meglumine Gd-DOTA). The HPLC-ICP-MS method used for the speciation study was first optimised for the separation of these three compounds. Fig. 2 shows the chromatogram of a standard solution containing 50 μg L^{-1} of the three GBCAs, with separation of the analytes within 8 min.

Prior to HPLC-ICP-MS analysis, wastewater sample treatment involved pre-concentration of GBCAs through evaporation under mild conditions followed by filtration, whereas seawater samples were treated by SPE. Because of the high salinity of the seawater matrix, SPE was used to remove salts that would interfere with the speciation analysis. Before treating the real samples, the SPE method was optimised for GBCA recovery, with particular attention to sample pH. Recovery tests were performed at four pH values in a synthetic seawater matrix with a salinity of 35; Table 1 reports the recoveries obtained for Gd-HP-DO3A and Gd-DOTA.

Analyte recovery during SPE was strongly pH dependent (Table 1). Gd-HP-DO3A showed high recoveries at pH values equal to or higher than 4, whereas recovery decreased to 53.2% at pH 3. Gd-DOTA showed the opposite behaviour, with maximum recovery at pH 3 and progressively lower recovery at higher pH, reaching 30.9% at pH 8. Recoveries for the linear contrast agent Gd-DTPA were below 40%. Based on the data in Table 1, pH 4 was selected for the seawater samples as a compromise for efficient recovery of both Gd complexes.

3.3. Total Gd and GBCAs in wastewater

Raw and treated wastewater samples from the Servola WWTP (see Study area section) were analysed for total gadolinium and its speciation. The results are reported in Table S1. Total Gd was quantified in all samples, with mean concentrations of 41.60 ± 27.83 ng L^{-1} and 32.83 ± 24.72 ng L^{-1} in raw and treated wastewater, respectively. Higher total Gd concentrations were observed in August 2023 in both raw and treated wastewater, whereas lower and comparable values were measured in October and December (Fig. 3).

Speciation analysis revealed the presence of Gd-HP-DO3A and Gd-DOTA in all wastewater samples, with Gd-HP-DO3A as the predominant compound (Table S1). In contrast, the linear GBCA Gd-DTPA was never detected above the detection limit. Gd-HP-DO3A had a mean concentration of 27.55 ± 22.51 ng L^{-1} in raw wastewater, with the highest value in August (51.69 ng L^{-1}) and the lowest in December (7.14 ng L^{-1}). In treated wastewater, the mean concentration was 21.65 ± 18.86 ng L^{-1}, with the highest value again in August (42.29 ng L^{-1}) and the lowest in December (5.3 ng L^{-1}). Gd-DOTA occurred at much lower concentrations, with mean contents of 0.80 ± 0.36 ng L^{-1} in raw wastewater and 0.52 ± 0.24 ng L^{-1} in treated wastewater. Its distribution among sampling campaigns differed from that of Gd-HP-DO3A: maximum Gd-DOTA concentrations occurred in December (1.03 and 0.80 ng L^{-1} in raw and treated wastewater, respectively), while minimum values of 0.38 ng L^{-1} occurred in October for raw wastewater and in August and October for treated wastewater (Table S1).

Total Gd concentrations decreased modestly after WWTP treatment, with a mean removal efficiency of 24% (Fig. 3 and Table 2). Gd-HP-DO3A showed a comparable mean removal of 24%. The mean removal of Gd-DOTA was 28%, but values varied more among

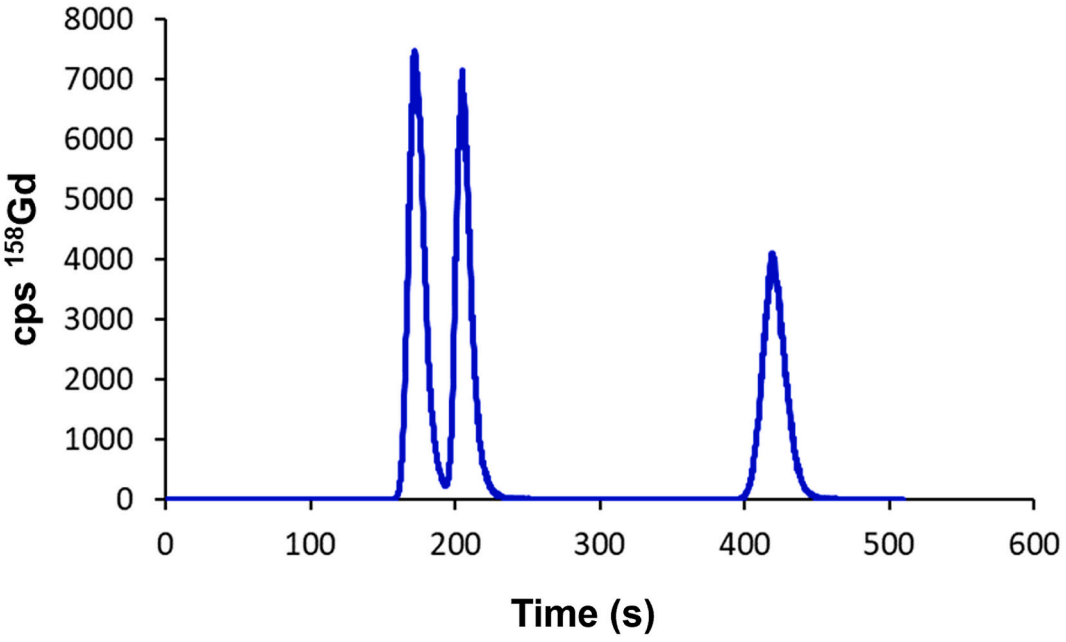

Fig. 2. Chromatogram of a 50 μg L^{-1} standard solution; elution order: Gd-HP-DO3A, Gd-DOTA, Gd-DTPA.

Table 1
Recoveries, expressed as %, for Gd-HP-DO3A and Gd-DOTA at four different pHs from a synthetic seawater with a salinity of 35.

pH	Gd-HP-DO3A	Gd-DOTA
3	53.2	81.6
4	79.0	75.4
6	86.6	56.2
8	92.8	30.9

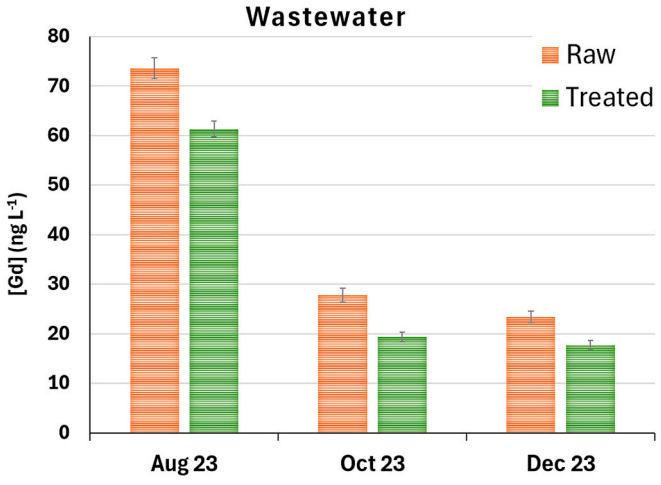

Fig. 3. Total gadolinium content in raw and treated wastewater collected between August and December 2023.

Table 2
Gd removal (%) attributable to the WWTP treatment system.

	Aug 23	Oct 23	Dec 23	Mean	SD
Gd TOT	17	30	24	24	7
Gd-HP-DO3A	18	27	26	24	5
Gd-DOTA	62	0	22	28	31
Other Gd	11	58	24	31	24

campaigns (Table 2); Gd-DOTA concentrations were consistently in the sub-ng L^{-1} range and much lower than those of the other analytes.

Comparison of total Gd with the summed concentrations of the GBCAs detected in each wastewater sample showed that gadolinium-based contrast agents made the major contribution to total Gd, except in samples collected in December 2023, when GBCA concentrations were low (Fig. 4 and Table 3). Anthropogenic gadolinium (Gd_{anth}) was calculated from the REE patterns (Table S2) using the methodology suggested by Brünjes et al., 2016 as reported in the note of Table S2.

Marked temporal differences in total Gd and GBCA concentrations were observed among the three wastewater sampling campaigns. To evaluate potential drivers, antecedent rainfall and seasonal population changes were examined using publicly available daily precipitation records from ARPA FVG – Regional Meteorological Observatory (OSMER), 2025 (Table S3) and monthly tourism statistics obtained by Regione Autonoma Friuli Venezia Giulia, 2025 (Table S4). Antecedent rainfall differed markedly among campaigns: October was the driest period and December the wettest. Total Gd and Gd-HP-DO3A concentrations nevertheless peaked in August. Tourist attendance also increased during summer, but accounted for only 2–3% of the 190,000 population equivalents served by the plant.

3.4. Total Gd and GBCAs in seawater

Total Gd concentrations in seawater ranged from 2.14 to 40.87 ng L^{-1} (Fig. 5 and Table S5), with an overall mean of 17.22 ± 9.18 ng L^{-1}. Concentrations varied markedly among sampling campaigns and stations, with the highest values generally at sites 0D and 0M along the submarine diffuser. At these stations, concentrations increased markedly in December, and pronounced differences occurred between surface and bottom waters, particularly at 0D, where the bottom water value was the overall maximum. In contrast, the reference station MA2_11 showed limited temporal variability and a homogeneous distribution between surface and bottom layers.

Results for Gd-HP-DO3A and Gd-DOTA are reported in Tables S6 and S7, respectively, whereas Gd-DTPA was never found above the detection limit. Gd-HP-DO3A was the predominant detected GBCA in all seawater samples (Fig. 6), with mean concentrations of 1.68 ± 0.09 ng L^{-1} in August, 1.71 ± 0.10 ng L^{-1} in October and 0.97 ± 0.49 ng L^{-1} in December. Gd-DOTA was above the LOD but at concentrations much

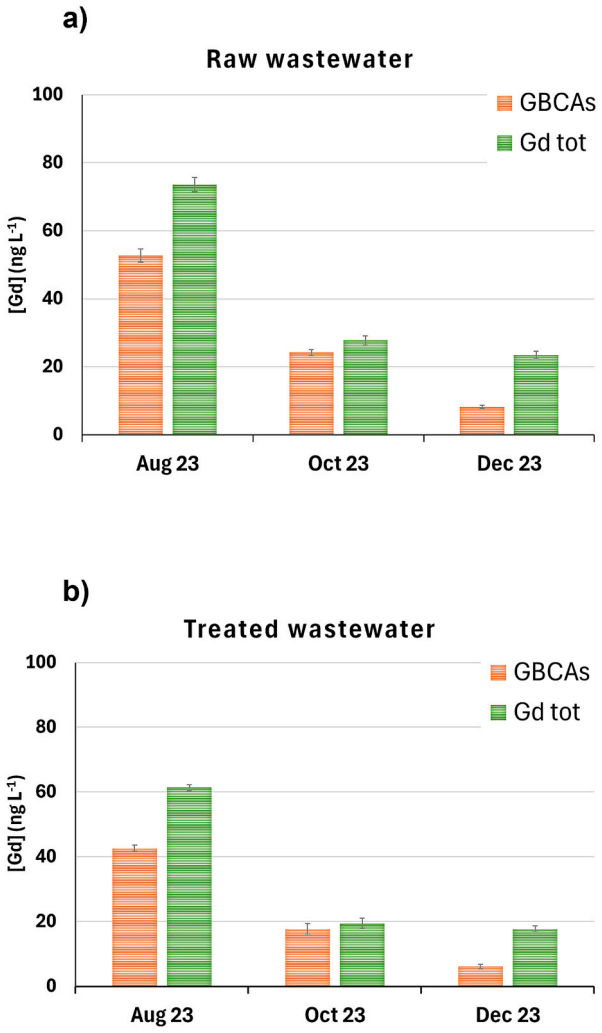

Fig. 4. Comparison between the concentration of total Gd and the sum of the GBCAs in a) raw wastewater and b) treated wastewater.

Table 3
Contribution (%) of GBCAs to total Gd in wastewater.

	Aug 23	Oct 23	Dec 23	Mean	SD
Raw wastewater					
Gd-HP-DO3A + Gd-DOTA	71.5	87.2	34.9	64.5	26.9
Gd-HP-DO3A	70.2	85.8	30.5	62.2	28.5
Gd-DOTA	1.3	1.4	4.4	2.4	1.8
Other Gd (Tot Gd - (Gd-HP-DO3A + Gd-DOTA)	28.5	12.8	65.1	35.5	26.9
Treated wastewater					
Gd-HP-DO3A + Gd-DOTA	69.6	91.5	34.4	65.2	28.8
Gd-HP-DO3A	68.9	89.6	29.9	62.8	30.3
Gd-DOTA	0.6	2.0	4.5	2.4	2.0
Other Gd (Tot Gd - (Gd-HP-DO3A + Gd-DOTA)	30.4	8.5	65.6	34.8	28.8

lower than Gd-HP-DO3A, with a pattern similar to that of wastewater. The summed detected GBCAs accounted for only a minor fraction of total Gd in seawater. Gd-HP-DO3A contributed 1–30%, except in the surface sample collected at station 0D in August 2023, where it reached 76% (Fig. S4a); Gd-DOTA contributed less than 16% in every sample (Fig. S4b).

'Other Gd', defined as the difference between total Gd and the detected GBCAs, was the dominant fraction in most seawater samples, accounting for 63–98% of total Gd. The exception was the surface sample collected at station 0D in August, where Other Gd accounted for 8% (Fig. S4c). Its contribution varied markedly among campaigns and was lowest (≤63%) in August at stations 0M and 0D, where the combined contribution of detected GBCAs was highest (37–92%) as reported in Fig. S4a,b; Gd-HP-DO3A concentrations in the treated WWTP effluent were also highest in August. In December, Other Gd increased to 92–98% at all stations and depths, while the combined detected GBCA contribution fell to 2–8%, with no appreciable differences between the stations along the submarine diffuser and MA2_11 (Fig. S4a,b). Despite the lower GBCA contribution in both the treated WWTP effluent and seawater in December, the highest total Gd concentrations occurred at stations 0M and 0D. Comparable total Gd peaks were not observed at the reference station MA2_11.

The December campaign followed the highest cumulative rainfall and persistent wind forcing. During the week before sampling, winds were consistently moderate to strong and originated from different sectors before shifting to strong ENE winds during the final two days (ARPA FVG – Regional Meteorological Observatory (OSMER), 2025) as reported in Table S8. Vertical profiles showed reduced salinity and elevated turbidity throughout the water column (Fig. S5). Gd_{anth} values estimated from the REE patterns are reported in Table S2. Gd_{anth} was higher than the sum of Gd-HP-DO3A and Gd-DOTA in all but one sample: the 0D surface sample collected in August, for which estimated anthropogenic Gd was very low and the Gd anomaly was absent from the pattern.

4. Discussion

4.1. Gd anomalies and evidence of anthropogenic inputs

Contamination by anthropogenic gadolinium has been recognised as an environmental issue since 1996, when significant Gd anomalies were first reported in surface waters in Germany (Bau and Dulski, 1996). The positive Gd anomaly is widely used to assess contamination in aquatic systems, especially freshwater environments, because deviation of Gd concentration from the natural rare-earth-element pattern indicates an anthropogenic source. Accordingly, anomaly in raw, treated wastewater and seawater found in almost all analysed samples, indicates an anthropogenic contribution.

The correspondence between the stronger August anomaly and the higher Gd concentrations, compared to October and December, supports this interpretation. However, REE patterns in wastewater are often difficult to define because REE concentrations are at trace to ultra-trace levels, the matrices are complex and variable, and REEs partition between dissolved and particulate-bound phases. These factors may distort the natural REE pattern and mask a positive anomaly associated with anthropogenic Gd. Similar behaviour has been already reported in the literature for river water (Kumasaka et al., 2024). In seawater, the anomaly may not always be evident due to the low Gd concentrations that are typically in the ng L^{-1} range. Wastewater effluents without a clear Gd anomaly have likewise been reported by Verplanck et al. (2005) and Rabiet et al. (2009), and absent or very weak anomalies have been reported in coastal seawater (da Costa et al., 2021; Ogata and Terakado, 2006; Pedreira et al., 2018). The low intensity anomaly also explains why Gd_{anth} was not higher than the summed detected GBCAs in some wastewater samples. The same limitation is evident in the 0D surface sample collected in August, where the absence of a Gd anomaly produced a very low estimate of anthropogenic gadolinium.

4.2. Speciation analyses and pH-dependent GBCA recovery in seawater

The speciation study focused on GBCAs because their use in medical MRI procedures has been identified as the main source of anthropogenic

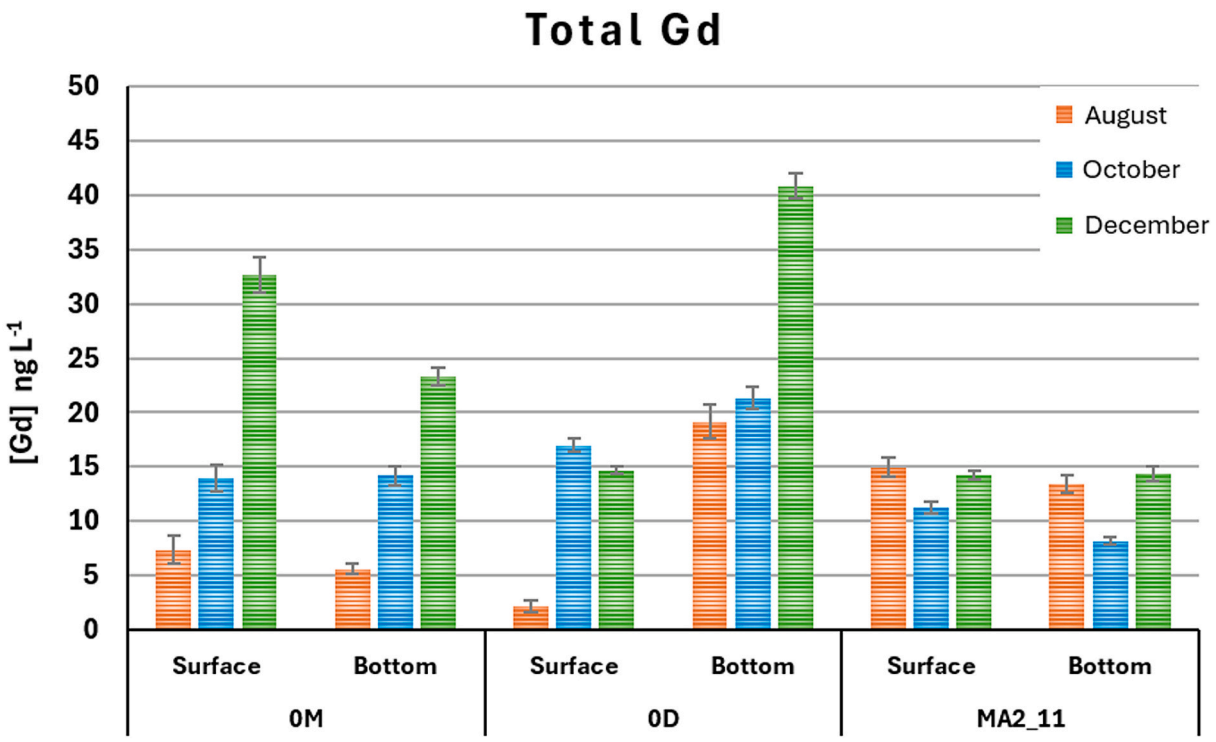

Fig. 5. Total gadolinium concentrations in seawater sampled along the submarine outfall (stations 0 M and 0D) and in the reference station (MA2_11).

Gd. The two macrocyclic compounds, Gd-HP-DO3A and Gd-DOTA, are currently among the most widely used GBCAs in MRI (Kraemer et al., 2024) because of their very high stability and consequent safety. The linear Gd-DTPA complex was retained as a target because it was widely used in the past, although its use in the EU is now restricted to intra-articular injection and banned for routine intravenous administration (European Medicines Agency, 2017).

The strong pH dependence of SPE recovery in the seawater matrix reflects the charge behaviour of the complexes. GBCAs may be neutral or carry a net negative charge depending on solution pH and may therefore interact repulsively with negatively charged groups on the activated carbon in the SPE cartridge. The reduced Gd-HP-DO3A recovery at pH 3 was probably caused by degradation of the contrast agent. Gd-DOTA contains four carboxylic groups, three of which coordinate Gd^{3+}, while the uncoordinated group undergoes protonation/deprotonation as pH changes. At higher pH, the dissociated form becomes predominant, increasing repulsive interactions with the adsorbent and producing poor Gd-DOTA retention and recovery. The low recovery of Gd-DTPA (< 40%) was probably caused by complex dissociation driven by competition from Mg and Ca (Schijf and Christy, 2018).

4.3. *Wastewater occurrence, treatment removal and temporal variability*

Total Gd concentrations in treated wastewater from the Servola WWTP were lower than those reported for most wastewater treatment plants (Table S9), mean values at many WWTPs worldwide were more than threefold higher. These comparisons should be interpreted in light of the broad time span covered by the literature and differences in plant size, treatment efficiency and the population equivalents served, all of which influence Gd concentrations in wastewater effluent.

The modest reduction in total Gd after treatment is consistent with previous findings (Telgmann et al., 2012; Turcotte et al., 2022; Bringas et al., 2024). The comparable mean removal of total Gd and Gd-HP-DO3A, together with the limited mean removal of Gd-DOTA, indicates that even a full-scheme wastewater treatment system including tertiary treatment may not fully prevent Gd release to the environment. The observed reductions probably reflect a combination of limited adsorption onto activated sludge, association with particulate matter removed during clarification and sedimentation, and possible transformation of some GBCAs. Because most GBCAs are highly stable and persistent, however, conventional wastewater treatment generally removes them only to a limited extent (Telgmann et al., 2012; Brünjes and Thilo Hofmann, 2020; Laczovics et al., 2023).

The interpretation of the apparent variability in Gd-DOTA removal requires particular caution. At consistently sub-ng L^{-1} concentrations, very small absolute differences between raw and treated wastewater translate into large percentage changes. The observed fluctuations in Gd-DOTA removal therefore do not provide robust evidence of temporal changes in WWTP removal performance.

Few studies have quantified individual GBCAs in WWTP wastewater. Telgmann et al. (2012) identified Gd-BT-DO3A as the main complex in raw and treated wastewater from a plant in Münster, Germany, accounting for 80% of total GBCAs, whereas Gd-DTPA and Gd-DOTA were present at much lower levels. Côme et al. (2026) reported Gd-DOTA concentrations above 600 ng L^{-1} in the effluent of a WWTP in Baudreix, France. To the best of our knowledge, the present study provides the first quantification of Gd-HP-DO3A in both raw and treated municipal wastewater. Nevertheless, detection of Gd-HP-DO3A and Gd-DOTA in surface waters near urban areas worldwide demonstrates their widespread use. For example, Gd-DOTA was detected in concentrations of about 89 ng L^{-1} in the river waters downstream the city of Berlin (Kesava Raju et al., 2010), even up to 838 ng L^{-1} near Münster, where high amounts of Gd-HP-DO3A were also observed (Macke et al., 2021). Among other GBCAs, Gd-DOTA and Gd-HP-DO3A were also detected in surface waters of the Muki River, Japan, where Gd-DOTA reached concentrations up to 39 ng L^{-1}, while Gd-HP-DO3A was below the detection limit (Okabayashi et al., 2021).

Overall, results highlighted marked temporal differences in the concentrations of total Gd and GBCAs among the three wastewater sampling campaigns. In this context, it is well known that municipal wastewater influent composition in influenced by temporal and spatial variations in water use by residential, commercial and industrial users,

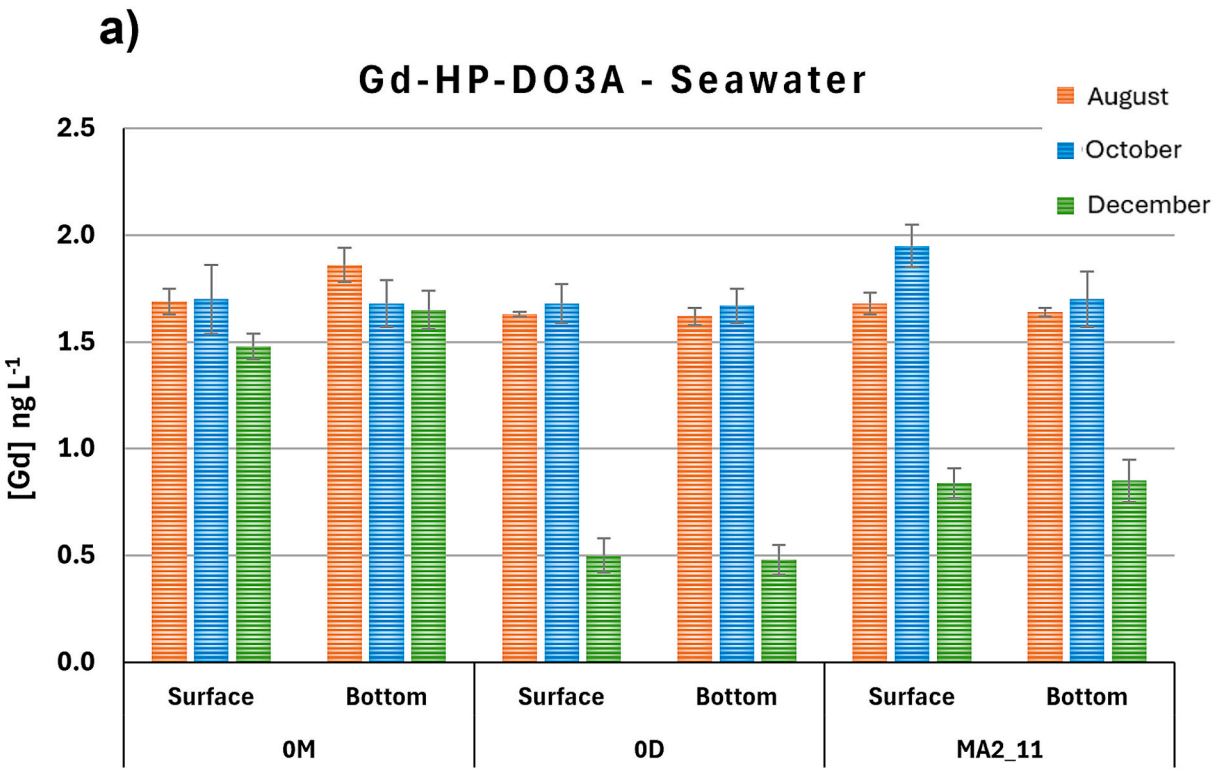

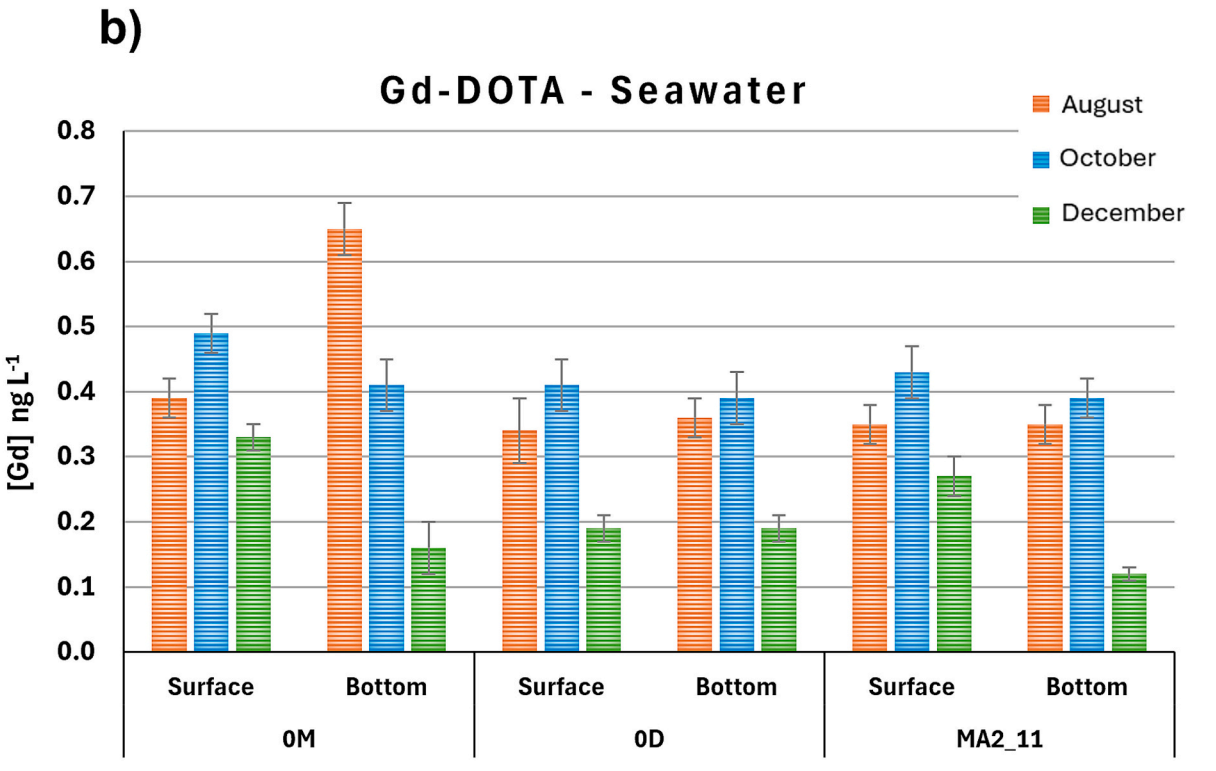

Fig. 6. Concentration of a) Gd-HP-DO3A and b) Gd-DOTA in seawater samples collected in August 2023, October 2023 and December 2023.

the structural complexity of sewer networks, and hydrometeorological conditions (El-Dakhakhni et al., 2026; Gao et al., 2023). Previous Gd studies have reported daily changes related to GBCA administration, patient excretion and sewer transport (Laczovics et al., 2023), as well as differences among sampling periods associated with hospital activity within a WWTP catchment (Bringas et al., 2024).

Rainfall was unlikely to be the main control on raw wastewater GBCA concentrations during this study because total Gd and Gd-HP-DO3A peaked in August rather than during the driest campaign. The lower GBCA contribution in December is nevertheless consistent with dilution and changes in wastewater composition caused by increased rainfall. Because the Servola WWTP receives combined sewer inflow, the substantial rainfall before the December campaign (see Table S3) increased runoff, diluted the wastewater stream and reduced the relative GBCA contribution to total Gd. The small tourist contribution to plant loading likewise cannot explain the pronounced August Gd peak. Rainfall and tourism are therefore better viewed as proxies for broader seasonal changes in wastewater influent characteristics than as direct drivers of GBCA occurrence.

The elevated August Gd concentrations probably reflect a combination of seasonal GBCA consumption, changes in wastewater composition and hydrological conditions, but the individual contributions cannot be resolved with the available dataset. Temporal changes in influent composition and loading may also contribute to the apparent differences in Gd-DOTA removal and are more plausible than substantial changes in the intrinsic performance of the treatment process.

4.4. Seawater distribution, local processes and environmental implications

The highest seawater Gd concentrations in the Gulf of Trieste (GoT) were comparable to values reported for coastal sites near WWTP outfalls in San Francisco Bay (Hatje et al., 2016) and in Osaka and Tokyo bays (Ogata and Terakado, 2006; Nozaki et al., 2000) as reported in Table S10. Most other studies reported lower concentrations, including work in Todos os Santos Bay and along the Bahia coast (Andrade et al., 2020; Pedreira et al., 2018) and in the German Bight (Ponnurangam et al., 2016) (Table S10). Relative to oceanic waters, total Gd concentrations in the GoT were up to sevenfold higher (Table S5).

For what concerns GBCAs, the absence of Gd-DTPA from seawater may reflect its limited stability in this matrix. Potential processes include transmetallation with other REEs or metals such as iron, competition with other organic ligands, formation of dinuclear Mg and Ca complexes, and continued Gd-DTPA dissociation as released Gd is removed by scavenging (Schijf and Christy, 2018).

The December peaks of total Gd at 0M and 0D were primarily associated with the Other Gd fraction, suggesting that additional processes affected this fraction within the wastewater discharge area. The reduced salinity and elevated turbidity measured after heavy rainfall and persistent winds are consistent with freshwater inputs, enhanced water-column mixing and increased suspended particulate matter. Under these conditions, mobilisation and redistribution of Other Gd may have contributed to the elevated total Gd near the submarine diffuser. The absence of comparable peaks at MA2_11 indicates that meteorological forcing alone cannot explain the distribution; rather, it may have promoted remobilisation of a local Other Gd fraction around the diffuser.

Although total Gd concentrations allow comparison among marine environments, the environmental behaviour and long-term stability of the GBCAs responsible for Gd anomalies remain poorly understood. Their long-term fate may include microbial transformation into other Gd-containing organic species or release of free Gd^{3+} ions through reactions with competing metal ions (Zhang et al., 2024). The lack of specific studies concerning the presence and diffusion of GBCAs in seawater makes it difficult to fully comprehend the anthropogenic impact on these complex aquatic ecosystems, highlighting the importance of speciation investigation of these emerging contaminants in marine environments.

5. Conclusions

This study provides the first evidence of the occurrence of macrocyclic gadolinium-based contrast agents (GBCAs) in Mediterranean seawater and demonstrates their persistence from wastewater to the receiving coastal environment. Gd-HP-DO3A was identified as the predominant GBCA in both municipal wastewater and receiving marine waters. Substantial “Other Gd” fraction in seawater points to geogenic inputs and unmonitored macrocyclic contrast agents. The limited removal of GBCAs during advanced wastewater treatment confirms wastewater effluents as a continuous source of anthropogenic gadolinium. Furthermore, the optimised SPE–HPLC-ICP-MS method proved suitable for the speciation of GBCAs in high-salinity seawater, providing a valuable analytical tool for environmental monitoring. These findings improve the current understanding of the environmental fate of GBCAs and support the use of anthropogenic gadolinium as a tracer of wastewater-derived contamination in Mediterranean coastal ecosystems.

CRediT authorship contribution statement

Claudia Stevanin: Writing – original draft, Visualization, Investigation, Conceptualization. **Tatiana Chenet:** Writing – original draft, Visualization, Investigation, Conceptualization. **Elena Ciuffreda:** Investigation, Data curation. **Cinzia Fabbro:** Writing – review & editing, Visualization, Methodology. **Mirco Cescon:** Investigation, Data curation. **Michele Giani:** Writing – review & editing. **Valentina Costa:** Investigation, Data curation. **Luisa Pasti:** Writing – review & editing, Supervision, Resources, Project administration, Funding acquisition.

Declaration of competing interest

The authors declare that they have no known competing financial interests or personal relationships that could have appeared to influence the work reported in this paper.

Acknowledgments

The authors acknowledge AcegasApsAmga S.p.A. (HERA Group), operator of the Servola wastewater treatment plant, for supporting the research activities on emerging contaminants presented in this study. This study was funded by the University of Ferrara (FAR 2025). The authors also acknowledge Antonella Pagnoni of the Department of Environmental and Prevention Sciences of the University of Ferrara for technical support.

Appendix A. Supplementary data

Supplementary data to this article can be found online at https://doi.org/10.1016/j.marpolbul.2026.120338.

Data availability

Data will be made available on request.

References

Altomare, A.J., Young, N.A., Beazley, M.J., 2020. A preliminary survey of anthropogenic gadolinium in water and sediment of a constructed wetland. J. Environ. Manag. 255, 109897. https://doi.org/10.1016/j.jenvman.2019.109897.

Amorim, A.M., Sodré, F.F., Rousseau, T.C.C., Maia, P.D., 2019. Assessing rare-earth elements and anthropogenic gadolinium in water samples from an urban artificial lake and its tributaries in the Brazilian Federal District. Microchem. J. 148, 27–34. https://doi.org/10.1016/j.microc.2019.04.055.

Andrade, R.L.B., Hatje, V., Pedreira, R.M.A., Böning, P., Pahnke, K., 2020. REE fractionation and human Gd footprint along the continuum between Paraguaçu

River to coastal South Atlantic waters. Chem. Geol. 532, 119303. https://doi.org/10.1016/j.chemgeo.2019.119303.
Andrade, M., Soares, A.M.V.M., Solé, M., Pereira, E., Freitas, R., 2023. Gadolinium accumulation and its biochemical effects in *Mytilus galloprovincialis* under a scenario of global warming. Environ. Sci. Pollut. Res. Int. 30, 116120–116133. https://doi.org/10.1007/s11356-023-30439-2.
ARPA FVG – Regional Meteorological Observatory (OSMER), 2025. Daily precipitation data from the regional meteorological network (Cattinara and Molo Fratelli Bandiera stations). In: Available at: ARPA FVG – Meteo e Clima Data Portal.
Bau, M., Dulski, P., 1996. Anthropogenic origin of positive gadolinium anomalies in river waters. Earth Planet. Sci. Lett. 143, 245–255. https://doi.org/10.1016/0012-821X(96)00127-6.
Bringas, A., Bringas, E., Ibañez, R., San Román, M.F., 2024. Tracing Gadolinium levels throughout wastewater treatment: insights from a yearly assessment in northern Spain. Sci. Total Environ. 948, 174819. https://doi.org/10.1016/j.scitotenv.2024.174819.
Brünjes, R., Thilo Hofmann, T., 2020. Anthropogenic gadolinium in freshwater and drinking water systems. Water Res. 182, 115966. https://doi.org/10.1016/j.watres.2020.115966.
Brünjes, R., Bichler, A., Hoehn, P., Lange, F.T., Brauch, H.-J., Hofmann, T., 2016. Anthropogenic gadolinium as a transient tracer for investigating river bank filtration. Sci. Total Environ. 571, 1432–1440. https://doi.org/10.1016/j.scitotenv.2016.06.105.
Côme, J., Bueno, M., Karamanis, P., Pannier, F., Mounicou, S., 2026. Simultaneous speciation of iodine-, gadolinium-, and platinum-based pharmaceuticals by HILIC-ICP-MS and its application to wastewaters. Talanta 298 (part B), 128974. https://doi.org/10.1016/j.talanta.2025.128974.
Comici, C., Bussani, A., 2007. Analysis of the River Isonzo discharge (1998-2005). Boll. Geofis. Teor. Appl. 48, 435–454.
da Costa, A.R.B., Rousseau, T.C.C., Maia, P.D., Amorim, A.M., Sodré, F.F., Teixeira, C.E. P., 2021. Anthropogenic gadolinium in estuaries and tropical Atlantic coastal waters form Fortaleza, Northeast Brazil. Appl. Geochem. 127, 104908. https://doi.org/10.1016/j.apgeochem.2021.104908.
Covelli, S., Pisoni, C., Pavoni, E., Floreani, F., Petranich, E., Adami, G., Deponte, M., Gordini, E., Dal Cin, M., Busetti, M., 2025. Lithogenic and anthropogenic contributions of trace metal(oid)s in coastal sediments near the Port of Trieste (northern Adriatic Sea): a geochemical normalisation approach based on regional background values. Mar. Pollut. Bull. 214, 117774. https://doi.org/10.1016/j.marpolbul.2025.117774 (ISSN 0025-326X).
Cozzi, S., Falconi, C.F., Comic'i, C., Čermelj, B., Kovac, N., Turk, V., Giani, M., 2012. Recent evolution of river discharges in the Gulf of Trieste and their potential responses to anthropogenic pressure and climate change. Estuar. Coast. Shelf Sci. 115, 14–24. https://doi.org/10.1016/j.ecss.2012.03.005.
Cozzi, S., Mistaro, A., Sparnocchia, S., Colugnati, L., Bajt, O., Toniatti, L., 2014. Anthropogenic loads and biogeochemical role of urea in the Gulf of Trieste. Sci. Total Environ. 493, 271–281. https://doi.org/10.1016/j.scitotenv.2014.05.148.
Cozzi, S., Cabrini, M., Kralj, M., De Vittor, C., Celio, M., Giani, M., 2020. Climatic and anthropogenic impacts on environmental conditions and phytoplankton community in the Gulf of Trieste (northern Adriatic Sea). Water 12, 2652. https://doi.org/10.3390/w12092652.
Ebrahimi, P., Barbieri, M., 2019. Gadolinium as an emerging microcontaminant in water resources: threats and opportunities. Geosciences 9 (2), 93. https://doi.org/10.3390/geosciences9020093.
El-Dakhakhni, O., Li, Z., Zhou, P., Snowling, S., 2026. Predicting wastewater influent characteristics using data-driven modeling approaches. Water 18, 1255. https://doi.org/10.3390/w18111255.
European Medicines Agency, 2017. EMA's final opinion confirms restrictions on use of linear gadolinium agents in body scans. https://www.ema.europa.eu/.
Faganeli, J., Falnoga, I., Klun, K., Mazej, D., Mozetič, P., Zuliani, T., Kovač, N., 2023. Metal(loid)s in suspended particulate matter and plankton from coastal waters (Gulf of Trieste, northern Adriatic Sea). J. Soils Sediments 23, 4085–4097. https://doi.org/10.1007/s11368-023-03519-6.
Falcieri, F.M., Kantha, L., Benetazzo, A., Bergamasco, A., Bonaldo, D., Barbariol, F., Malačič, V., Sclavo, M., Carniel, S., 2016. Turbulence observations in the Gulf of Trieste under moderate wind forcing and different water column stratification. Ocean Sci. 12, 433–449. https://doi.org/10.5194/os-12-433-2016.
Fanelli, M., Girolametti, F., Truzzi, C., Illuminati, S., Ajdini, B., Susmel, S., Celussi, M., Šangulin, J., Annibaldi, A., 2022. Impact of depuration plants on nutrient levels in the North Adriatic Sea. Water 14 (12), 1930. https://doi.org/10.3390/w14121930.
Gao, Y., Shi, X., Jin, X., Wang, X.C., Jin, P., 2023. A critical review of wastewater quality variation and in-sewer processes during conveyance in sewer systems. Water Res. 228 (Part B), 119398. https://doi.org/10.1016/j.watres.2022.119398.
Gao, X., Han, G., Zhang, S., Ren, J., 2025. Anthropogenic gadolinium as an emerging contaminant in megacity rivers: sources, fluxes, and policy implications in North China. J. Environ. Manag. 395, 128014. https://doi.org/10.1016/j.jenvman.2025.128014.
Hatje, V., Bruland, K.W., Flegal, A.R., 2016. Increases in anthropogenic gadolinium anomalies and rare earth element concentrations in San Francisco Bay over a 20 year record. Environ. Sci. Technol. 50 (8), 4159–4168. https://doi.org/10.1021/acs.est.5b04322.
Hennebrüder, K., Wennrich, R., Mattusch, J., Stärk, H.-J., Engewald, W., 2004. Determination of gadolinium in river water by SPE preconcentration and ICP-MS. Talanta 63 (2), 309–316. https://doi.org/10.1016/j.talanta.2003.10.053.
Horstmann, M., Gonzalez De Vega, R., Bishop, D.P., Karst, U., Doble, P.A., Clases, D., 2021. Determination of gadolinium MRI contrast agents in fresh and oceanic waters of Australia employing micro-solid phase extraction, HILIC-ICP-MS and bandpass mass filtering. J. Anal. At. Spectrom. 36, 767–775. https://doi.org/10.1039/d0ja00493f.
Inoue, K., Fukushi, M., Sahoo, S.K., Veerasamy, N., Furukawa, A., Soyama, S., Sakata, A., Isoda, R., Taguchi, Y., Hosokawa, S., Sagara, H., Natarajan, T., 2022. Measurements and future projections of Gd-based contrast agents for MRI exams in wastewater treatment plants in the Tokyo metropolitan area. Mar. Pollut. Bull. 174, 113259. https://doi.org/10.1016/j.marpolbul.2021.113259.
Inoue, K., Natarajan, T., Isoda, R., Fukushi, M., Sahoo, S.K., 2025. Anthropogenic gadolinium contamination assessment in sewage, river, and tap water samples from the urban Osaka area, Japan. Sci. Total Environ. 975, 179255. https://doi.org/10.1016/j.scitotenv.2025.179255.
Kesava Raju, C.S., Cossmer, A., Scharf, H., Panne, U., Lück, D., 2010. Speciation of gadolinium based MRI contrast agents in environmental water samples using hydrophilic interaction chromatography hyphenated with inductively coupled plasma mass spectrometry. J. Anal. At. Spectrom. 25, 55–61. https://doi.org/10.1039/b919959d.
Kraemer, D., Schmidt, K., Klimpel, F., Rauch, U., Ernst, D.M., Paul, S.A.L., Haeckel, M., Koschinsky, A., Bau, M., 2024. Tracking the distribution of persistent and mobile wastewater-derived substances in the southern and central North Sea using anthropogenic gadolinium from MRI contrast agents as a far-field tracer. Mar. Pollut. Bull. 207, 116794. https://doi.org/10.1016/j.marpolbul.2024.116794.
Krohn, L.M., Klimpel, F., Béziat, P., Bau, M., 2024. Impacts of COVID-19 and climate change on wastewater-derived substances in urban drinking water: evidence from gadolinium-based contrast agents in tap water from Berlin, Germany. Water Res. 259, 121847. https://doi.org/10.1016/j.watres.2024.121847.
Krzyk, M., Drev, D., Batič, E., 2024. The concept of circular economy in wastewater management along the Slovenian coast. Kem. Ind. 73, 417–422. https://doi.org/10.15255/KUI.2023.053.
Kumasaka, S., Kartamihardja, A.A.P., Kumasaka, Y., Kameo, S., Koyama, H., Tsushima, Y., 2024. Anthropogenic gadolinium in the Tone River (Japan): an update showing a 7.7-fold increase from 1996 to 2020. Eur. Radiol. Exp. 8 (1), 64. https://doi.org/10.1186/s41747-024-00460-2.
Lachaux, N., Catrouillet, C., Marsac, R., Poirier, L., Pain-Devin, S., Gross, E.M., Giamberini, L., 2022. Implications of speciation on rare earth element toxicity: a focus on organic matter influence in Daphnia magna standard test. Environ. Pollut. 307, 119554. https://doi.org/10.1016/j.envpol.2022.119554.
Lachaux, N., Otero-Fariña, A., Minguez, L., Sohm, B., Rétif, J., Châtel, A., Poirier, L., Devin, S., Pain-Devin, S., Gross, E.M., Giamberini, L., 2023. Fate, subcellular distribution and biological effects of rare earth elements in a freshwater bivalve under complex exposure. Sci. Total Environ. 905, 167302. https://doi.org/10.1016/j.scitotenv.2023.167302.
Laczovics, A., Csige, I., Szabó, S., Tóth, A., Kálmán, F.K., Tóth, I., Fülöp, Z., Berényi, E., Braun, M., 2023. Relationship between gadolinium-based MRI contrast agent consumption and anthropogenic gadolinium in the influent of a wastewater treatment plant. Sci. Total Environ. 877, 162844. https://doi.org/10.1016/j.scitotenv.2023.162844.
Macke, M., Quarles, C.D., Sperling, M., Karst, U., 2021. Fast and automated monitoring of gadolinium-based contrast agents in surface waters. Water Res. 207, 117836. https://doi.org/10.1016/j.watres.2021.117836.
Malačič, V., Celio, M., Čermelj, B., Bussani, A., Comici, C., 2006. Interannual evolution of seasonal thermohaline properties in the Gulf of Trieste (northern Adriatic) 1991–2003. J. Geophys. Res. Oceans 111, C08009. https://doi.org/10.1029/2005JC003267.
Martino, C., Bonaventura, R., Byrne, M., Roccheri, M., Matranga, V., 2017. Effects of exposure to gadolinium on the development of geographically and phylogenetically distant sea urchins species. Mar. Environ. Res. 128, 98–106. https://doi.org/10.1016/j.marenvres.2016.06.001.
McLennan, S.M., 1989. Rare earth elements in sedimentary rocks: influence of provenance and sedimentary processes. In: Lipin, B.R., McKay, G.A. (Eds.), Geochemistry and Mineralogy of Rare Earth Elements.
Moreira, I., Pereira, E., Soares, A.M.V.M., Freitas, R., 2025. Gadolinium: a review on concentrations and impacts in marine and coastal systems. Environ. Pollut. 381, 126453. https://doi.org/10.1016/j.envpol.2025.126453.
Moreira, I., Cunha, M., Leite, C., Soares, A.M.V.M., Pereira, E., Freitas, R., 2026. Contrasting responses of *Ruditapes philippinarum* and *Mytilus galloprovincialis* to gadolinium and salinity stress. Aquat. Living Resour. 39, 5. https://doi.org/10.1051/alr/2025023.
Nozaki, Y., Lerche, D., Alibo, D.S., Tsutsumi, M., 2000. Dissolved indium and rare earth elements in three Japanese rivers and Tokyo Bay: evidence for anthropogenic Gd and in. Geochim. Cosmochim. Acta 64 (23), 3975–3982. https://doi.org/10.1016/S0016-7037(00)00472-5.
Ogata, T., Terakado, Y., 2006. Rare earth element abundances in some seawaters and related river waters from the Osaka Bay area, Japan: significance of anthropogenic Gd. Geochem. J. 40, 463–474. https://doi.org/10.2343/geochemj.40.463.
Okabayashi, S., Kawane, L., Mrabawani, N.Y., Iwai, T., Narukawa, T., Tsuboi, M., Chiba, K., 2021. Speciation analysis of gadolinium-based contrast agents using aqueous eluent-hydrophilic interaction liquid chromatography hyphenated with inductively coupled plasma-mass spectrometry. Talanta 222, 121531. https://doi.org/10.1016/j.talanta.2020.121531.
Oluwasola, I.E., Ahmad, A.L., Shoparwe, N.F., Ismail, S., 2022. Gadolinium based contrast agents (GBCAs): uniqueness, aquatic toxicity concerns, and prospective remediation. J. Contam. Hydrol. 250, 104057. https://doi.org/10.1016/j.jconhyd.2022.104057.
Pastorino, P., Ginebreda, A., 2021. Contaminants of emerging concern (CECs): occurrence and fate in aquatic ecosystems. Int. J. Environ. Res. Public Health 18 (24), 13401. https://doi.org/10.3390/ijerph182413401.

Pedreira, R.M.A., Pahnke, K., Böning, P., Hatje, V., 2018. Tracking hospital effluent-derived gadolinium in Atlantic coastal waters off Brazil. Water Res. 145, 62–72. https://doi.org/10.1016/j.watres.2018.08.005.

Pereto, C., Lerat-Hardy, A., Baudrimont, M., Coynel, A., 2023. European fluxes of medical gadolinium to the ocean: a model based on healthcare databases. Environ. Int. 173, 107868. https://doi.org/10.1016/j.envint.2023.107868.

Ponnurangam, A., Bau, M., Brenner, M., Koschinsky, A., 2016. Mussel shells of *Mytilus edulis* as bioarchives of the distribution of rare earth elements and yttrium in seawater and the potential impact of pH and temperature on their partitioning behavior. Biogeosciences 13, 751–760. https://doi.org/10.5194/bg-13-751-2016.

Querin, S., Crise, A., Deponte, D., Solidoro, C., 2007. Numerical study of the role of wind forcing and freshwater buoyancy input on the circulation in a shallow embayment (Gulf of Trieste, northern Adriatic Sea). J. Geophys. Res. 112 (C3), 1–19. https://doi.org/10.1029/2006JC003611.

Rabiet, M., Brissaud, F., Seidel, J.L., Pistre, S., Elbaz-Poulichet, F., 2009. Positive gadolinium anomalies in wastewater treatment plant effluents and aquatic environment in the Hérault watershed (South France). Chemosphere 75 (8), 1057–1064. https://doi.org/10.1016/j.chemosphere.2009.01.036.

Regione Autonoma Friuli Venezia Giulia, 2025. Flussi turistici dei Comuni della Regione dal 2022 [Dataset]. Catalogo Open Data Regione Friuli Venezia Giulia. https://www.dati.friuliveneziagiulia.it/Istruzione-cultura-e-sport/Flussi-turistici-dei-Comuni-della-Regione-dal-2022/7eps-cpgr.

Rogowska, J., Olkowska, E., Ratajczyk, W., Wolska, L., 2018. Gadolinium as a new emerging contaminant of aquatic environments. Environ. Toxicol. Chem. 37 (6), 1523–1534. https://doi.org/10.1002/etc.4116.

Savonitto, G., Comici, C., Lanzoni, A., Bussani, A., Brunetti, F., Gerin, R., 2025. Updated insights into the Isonzo River (NE Italy) flow rate in the 1998-2022 period. Bull. Geophys. Oceanogr. 66 (3), 317–330. https://doi.org/10.4430/bgo00496.

Scarciglia, A., Papi, C., Romiti, C., Leone, A., Di Gregorio, E., Ferrauto, G., 2025. Gadolinium-based contrast agents (GBCAs) for MRI: a benefit–risk balance analysis from a chemical, biomedical, and environmental point of view. Global Chall. 9 (3), 2400269. https://doi.org/10.1002/gch2.202400269.

Schijf, J., Christy, I.J., 2018. Effect of Mg and Ca on the stability of the MRI contrast agent Gd–DTPA in seawater. Front. Mar. Sci. 5, 111. https://doi.org/10.3389/fmars.2018.00111.

Shabani, M.B., Akagi, T., Masuda, A., 1992. Preconcentration of trace rare-earth elements in seawater by complexation with bis(2-ethylhexyl) hydrogen phosphate and 2-ethylhexyl dihydrogen phosphate adsorbed on a C18 cartridge and determination by inductively coupled plasma mass spectrometry. Anal. Chem. 64 (7), 737–743. https://doi.org/10.1021/ac00031a008.

Telgmann, L., Wehe, C.A., Birka, M., Künnenmeyer, J., Nowak, S., Sperling, M., Karst, U., 2012. Speciation and isotope dilution analysis of gadolinium-based contrast agents in wastewater. Environ. Sci. Technol. 46 (21), 11929–11936. https://doi.org/10.1021/es301981z.

Turcotte, P., Smyth, S.A., Gagné, F., Gagnon, C., 2022. Lanthanides release and partitioning in municipal wastewater effluents. Toxics 10 (5), 254. https://doi.org/10.3390/toxics10050254.

Verplanck, P.L., Taylor, H.E., Nordstrom, D.K., Barber, L.B., 2005. Aqueous stability of gadolinium in surface waters receiving sewage treatment plant effluent, Boulder Creek, Colorado. Environ. Sci. Techol. 39 (18), 6923–6929. https://doi.org/10.1021/es048456u.

Wysocka, I.A., Rogowska, A.M., Kostrz-Sikora, P., 2023. Investigation of anthropogenic gadolinium in tap water of polish cities: Gdańsk, Kraków, Warszawa, and Wrocław. Environ. Pollut. 323, 121289. https://doi.org/10.1016/j.envpol.2023.121289.

Zabrecky, J.M., Liu, X.M., Wu, Q., Cao, C., 2021. Evidence of anthropogenic gadolinium in triangle area waters, North Carolina, USA. Water 13 (14), 1895. https://doi.org/10.3390/w13141895.

Zhang, Z., Jiang, W., Gu, T., Guo, N., Sun, R., Zeng, Y., Han, Y., Yu, K., 2024. Anthropogenic gadolinium contaminations in the marine environment and its ecological implications. Environ. Pollut. 359, 124740. https://doi.org/10.1016/j.envpol.2024.124740.

Zhang, K., Zocher, A.-L., Bau, M., 2025. Rare earth element and yttrium behaviour during metabolic transfer and biomineralisation in the marine bivalve *Mytilus edulis*: evidence for a (partially) biological origin of REY anomalies in mussel shells. Sci. Total Environ. 958, 178056. https://doi.org/10.1016/j.scitotenv.2024.178056.

Zhang, K., Scharnweber, K., Riedel, J.A., Zocher, A.-L., Bau, M., 2026. Behavior of geogenic and anthropogenic rare earth elements and yttrium in a natural freshwater ecosystem. Water Res. 295, 125508. https://doi.org/10.1016/j.watres.2026.125508.